

Mechanical Properties of Zirconium Ceramics with Hierarchical Porous Structure

S Kulkov^{1,2,3}, E Shutilova¹, S Buyakova^{1,2,3}

¹Institute of Strength Physics and Materials Science SB RAS, 2/4, pr. Akademicheskii, Tomsk, 634055, Russia

²Tomsk Polytechnic University, 30, Lenin Avenue, Tomsk, 634050, Russia.

³Tomsk State University, 36, Lenin Avenue, Tomsk, 634050, Russia

Email: kulkov@ms.tsc.ru

Abstract. The work studies porous ceramics produced from ultra-fine powders. The porosity of ceramic samples was from 15 to 80%. The ceramic materials had cellular structure. A distinctive feature of all deformation diagrams obtained in the experiment was their nonlinearity at low deformations, which was described by the parabolic law. It was shown that the observed nonlinear elasticity for low deformations on deformation diagrams is due to mechanical instability of cellular elements in a ceramic frame.

1. Introduction

Today, the use of additive technologies in the production of structural and functional application of ceramics is a promising direction. Additive technologies allow producing objects of complex shape.

Ceramics based on partially stabilized zirconia are the most interesting among the variety of ceramic materials due to their inherent high fracture toughness because of transformation toughening phenomena. Their characteristics are known to be determined by the quality of source ceramic powder (particle shape, particle size distribution), the conditions of compaction and sintering modes and any features of each phase, and how these phases, including pores, are arranged in relation to each other. The most important factor in successful application of materials is understanding the features of a structure emerging in them and their behavior under mechanical impact.

Plasma spray synthesis and chemical co-precipitation methods are the main efficient routes of ultra-fine powder production for additive processes to obtain ceramics due to activation of sintering [1]. The sintering process for these powders with identical chemical composition may be very different, and the final structure of a sintered body depends on particle size, surface energy, strain conserved in the whole system, etc. [2]. For example, one can obtain hollow-ball particles, which shape will condition a special morphology structure of materials [3, 4].

The aim of the work is the investigation of densification, structure and mechanical properties of materials from zirconia-based powders produced by plasma spray synthesis and sintered at different temperatures.

2. Materials and experimental procedure

Ceramic samples made from plasma-sprayed and chemically precipitated (97 mol% ZrO₂ + 3 mol% Y₂O₃) powders were studied. To study densification kinetics, the samples were produced by pressing as-received powders till relative density of 0.33 and sintering at 1500 °C for up to 20 hours.



Structure investigation was carried out for the samples sintered in the temperature range 1400–1650 °C during isothermal holding for 1 to 5 hours after uniaxial compression with the loading speed of $4 \cdot 10^{-4} \text{ s}^{-1}$.

Phase identification and evaluation of coherently diffracted domains (CDD) were determined from X-ray diffractometry data [5, 6]. Scanning electron microscope observations operated at 20–30 kV were used to determine the structure and average grain and pore size.

3. Results and discussion

Zirconia powder was characterized by spherical particles and their agglomerates (Figure 1a). The average particle size was 1.5 μm . The specific surface of chemically precipitated powder was measured to be $7 \text{ m}^2/\text{g}$. According to the X-ray data, the tetragonal phases of ZrO_2 were predominant in the amount of 95% with an average CDD size of 20 nm. An average CDD size of monoclinic phase was equal to 20 nm.

Density dependencies during sintering process are represented in Figure 1b, and it can be concluded that most intensive densification occurred at the heating stage. The analysis of this dependence using equation $\Delta L/L = K \cdot \tau^n$ ($\Delta L/L$ is relative shrinkage, K is kinetic coefficient; n is constant of densification rate) in log-log coordinates revealed that n for the samples made from plasma-sprayed powder is twice as much as for the samples based on chemically precipitated powder: 0.1 and 0.04, respectively [7].

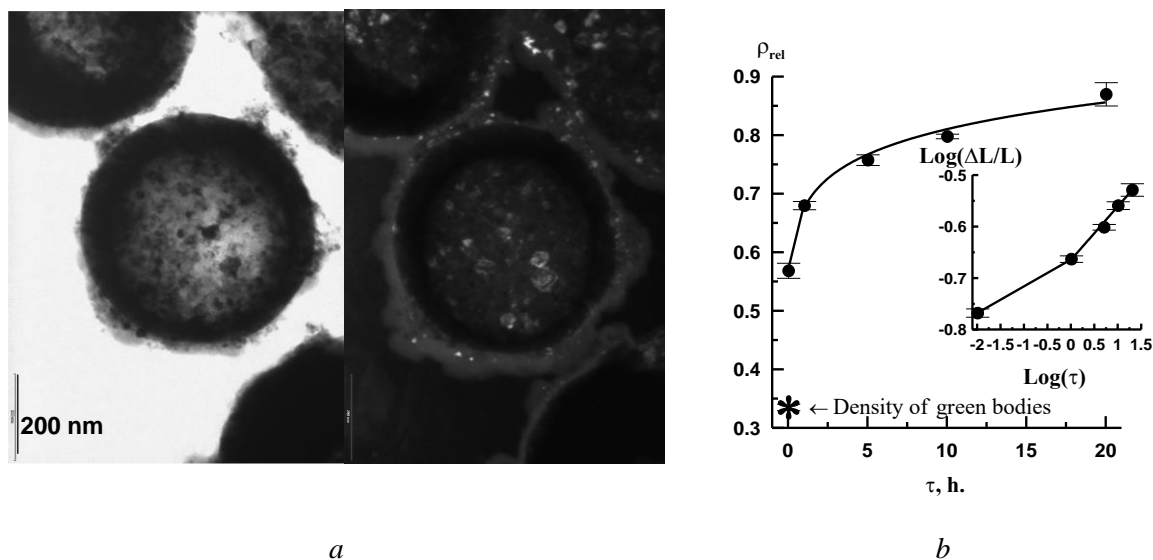


Figure 1. ZrO_2 powder synthesized by plasma-sprayed method: a) TEM image, bright and dark filed; b) dependencies of relative density on the duration of isothermal holding for ZrO_2 powder and kinetic dependences of samples shrinkage during isothermal holding.

X-ray analysis has shown that the tetragonal phase content in sintered ceramics was decreasing with the increase of the holding time up to 5 hours for materials based on plasma-sprayed powder from 95% down to 60%; further increase of holding time had no effect on the phase composition.

The structure of ceramic materials produced from plasma-sprayed ZrO_2 powder was represented as a system of cell and rod structure elements (Figure 2a). Cellular structure formed by stacking hollow-powder particles can be easily seen on the images of fracture surfaces of obtained ceramics. There were three types of pores in ceramics: large cellular hollow spaces, small interparticle pores which are not filled with powder particles and the smallest pores in the shells of cells. The cells generally had

irregular shape. The dimensions of the cells are far larger than the thickness of walls, which are presented by single-layer ZrO_2 grains.

The increase of the pore space in the ceramics was accompanied by the decrease of the average grain size. Quantity and the size of pores and the grain size in the materials produced by powder technology are highly dependent on thermokinetic sintering conditions (Figure 2b). Obviously, the increase in the volume of pores in the material from ~30% up to 80% was achieved by reducing the sintering temperature of the samples, and it was accompanied by an increase in the average size of large pores from 2 to 6 microns. Changing the porosity of the material had practically no influence on the average size of interparticle pores, the average size of which was 0.5 microns. It can be assumed that the presence of large pores close to a spherical shape in the tested ceramics is due to the presence of hollow spherical particles in source powders, since their average size is commensurate with the average size of large pores in the sintered material.

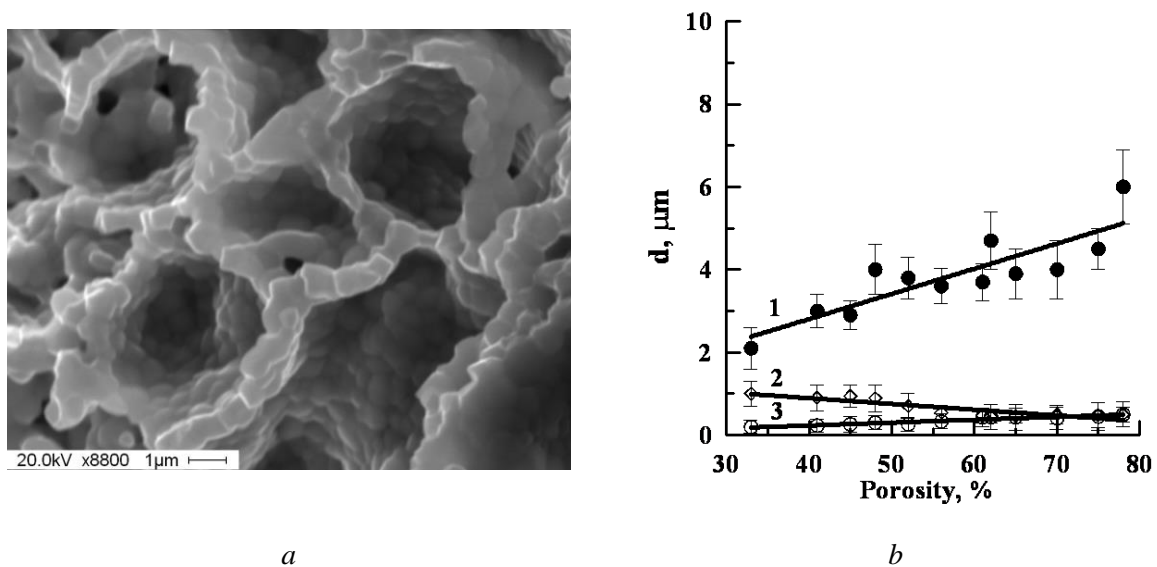


Figure 2. a) Fracture surface of sintered ceramic samples. Cellular structure of porous ceramics (porosity is 30%); b) The dependence of average size of the interior of the cells (1), of average size of grain (2) and of average size of small interparticle pores (3) on porosity.

Stress-strain diagram of porous ceramics, which were produced by plasma-sprayed method are presented in Figure 3a. The obtained stress-strain diagrams had descending branch with a monotonic decrease of stress. This is the evidence of damage accumulation in the samples in contrast to the stress-strain diagrams of brittle materials with a homogeneous structure. Microdamages appearing in the material has local nature and the sample under load retained the ability to resist increasing load. A distinctive feature of all the $\sigma - \varepsilon$ diagrams obtained in the experiment was their nonlinearity at low deformations which was described by the parabolic law. Cyclic loading of samples on the parabolic section of the diagrams did not reveal residual strain. Therefore, the nonlinearity in the stress-strain diagrams was due to the elastic deformation of ceramics with cellular structure.

Replotting deformation diagrams in $\ln - \ln$ coordinates allowed us to determine the exponent of the Hollomon equation [8] ($\sigma = K \varepsilon^n$, where σ is true stress; ε is true strain; n is parabolic index; K is constant for a given material, defined as a value of true stress for small true strain) from the experimental data. In this case, the index takes the value of the power function of the slope of the strain diagram in logarithmic scale (Figure 3b).

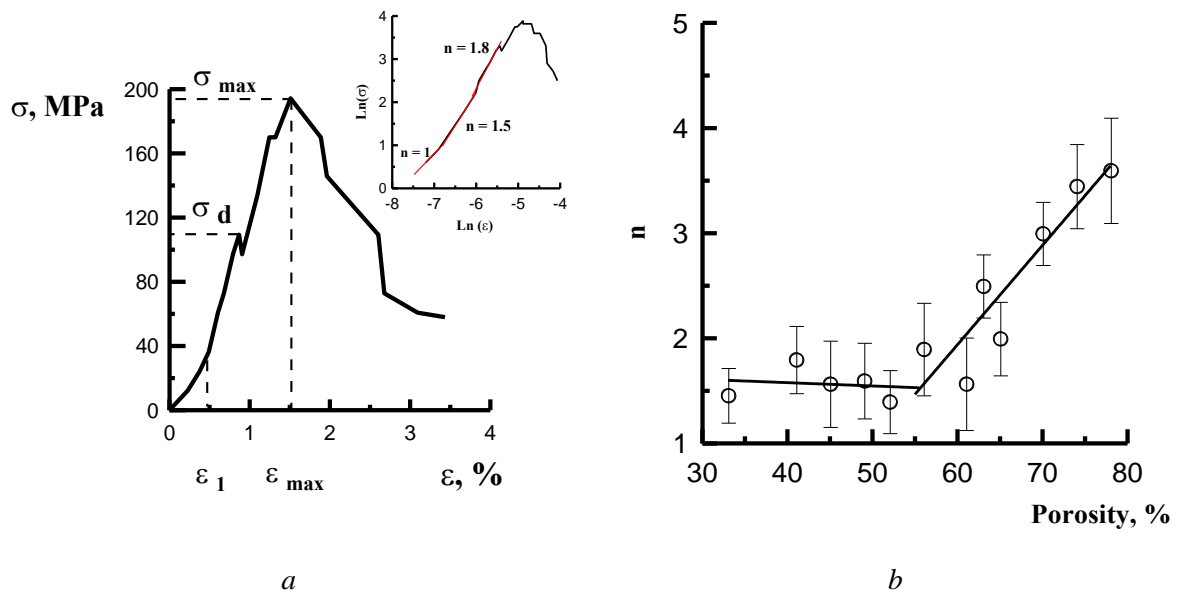


Figure 3. a) Stress-strain diagrams of ceramics compression with the porosity of 50%; b) the dependence of parabolic index from porosity.

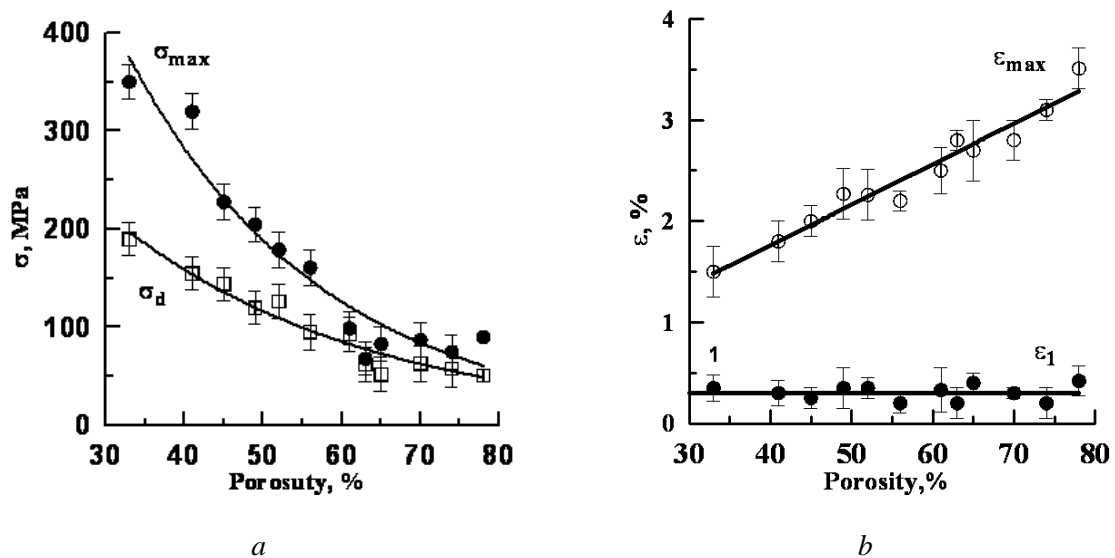


Figure 4. a) The dependence of maximum stress σ_{max} and the stress corresponding to emergence of microdamages in material σ_d from porosity; b) The dependence of strain corresponding to the end of the parabolic section on the rising branches of the stress-strain diagrams ε_1 and the strain corresponding to the maximum value of stress in ceramic samples ε_{max} from porosity.

The dependencies of maximum stress σ_{max} and the stress corresponding to the emergence of microdamages in material σ_d from porosity are presented in Figure 4a. Evidently, while the porosity decreases in the ceramics from 80% down to 30%, the maximum stress and the stress corresponding to the emergence of microdamages in material increased from 50 to 400 MPa and from 50 to 250 MPa, respectively. With the increase in the quantity of pores in the ceramics, the difference between the maximum stress and the stress corresponding to the emergence of microdamages decreased. When the

volume fraction of pores in the samples was more than 60%, σ_{\max} and σ_d were identical. Rising and descending branches of stress-strain diagrams became gentler.

The dependence of strain corresponding to the end of the parabolic section on the rising branches of the stress-strain diagrams ε_1 (1) and the strain corresponding to the maximum value of stress in ceramic samples ε_{\max} (2) from porosity are presented in Figure 4b. The increase of porosity from 30% up to 80% caused the increase of ε_{\max} from 1.5% to 3.5%. The obtained values of relative strain (up to ~3.5%) were significantly higher than values for nonporous ceramics. The increase of the porosity in ceramics had virtually no impact on the amount of strain ε_1 , which averaged to 0.5%.

4. Conclusion

It has been shown that the most intensive densification of studied materials took place during heating stage. In the stress-strain diagrams, the nonlinearity occurred due to the elastic deformation of ceramics with cellular structure. The character of the received strain-porosity dependences probably was a result of porosity type change.

It was shown that the “stress - strain” diagrams on the initial stage of deformation was nonlinear with high parabolic factor of strain-stress curves. It was shown that rod-like and/or cellular structures were formed in material, and the fracture of material occurred in the elastic area.

Acknowledgement

This work was financially supported by Tomsk State University Competitiveness Improvement Program and Siberian Branch Program #III.23.2.3.

References

- [1] Fedorchenko I M and Ivanova I I 1974 *About influence of particle size and specific surface on densification during the sintering* (Kiev: Naukova Dumka)
- [2] Gusev A I and Rempel A I 2001 *Nanocrystalline materials* (Moscow: PHYSMATHLIT)
- [3] Kulkov S N and Buyakova S P 2007 Structure, phase composition and technologies features of zirconia-based nanosystems *Russian Nanotechnology* **2** 1 119-132
- [4] Kalatur E, Buyakova S P and Kulkov S N 2014 Porosity and mechanical properties of zirconium ceramics *Epitoanyag - Journal of Silicate Based and Composite Materials* **66** 2 31-34.
- [5] Torayda H, Yoshimura M and Somiya S 1984 *J. Am. Ceram. Soc.* **67** 119-121
- [6] Gorelic S S, Skakov Yu A and Rastorguev L N 1994 *X-ray and electron/optical microscope analysis* (Moscow: MISIS)
- [7] Kulkov S N, Buyakova S P and Gomze L A 2014 Structure and mechanical properties of ZrO₂ – based systems *Epitoanyag - Journal of Silicate Based and Composite Materials* **66** 1 2-6.
- [8] Hertzberg R W 1989 *Deformation and fracture mechanics of engineering materials* (John Wiley and Sons, Inc.).